

Thermodynamic and Hydrodynamic Characteristics of Interacting System Formed in Relativistic Heavy Ion Collisions

Xu-Hong Zhang^{1,*}, Hao-Ning Wang^{2,†}, Fu-Hu Liu^{1,‡}, Khusniddin K. Olimov^{3,4,§}

¹*Institute of Theoretical Physics, State Key Laboratory of Quantum Optics and Quantum Optics Devices & Collaborative Innovation Center of Extreme Optics, Shanxi University, Taiyuan 030006, China*

²*College of Mechanical and Vehicle Engineering, Taiyuan University of Technology, Taiyuan 030024, China*

³*Physical-Technical Institute of Uzbekistan Academy of Sciences, Chingiz Aytmatov Street 2b, 100084 Tashkent, Uzbekistan*

⁴*Department of Natural Sciences, National University of Science and Technology MISIS (NUST MISIS), Almalyk Branch, 110105 Almalyk, Uzbekistan*

Abstract: To search for the energy of expected critical point of hadronic matter transition to quark-gluon plasma, based on the framework of a multi-source thermal model, we analyze the soft transverse momentum (p_T) spectra of the charged particles (π^- , π^+ , K^- , K^+ , \bar{p} , and p) produced in gold-gold (Au–Au) collisions at the center-of-mass energies $\sqrt{s_{NN}} = 7.7, 11.5, 14.5, 19.6, 27, 39, 62.4$, and 200 GeV from the STAR Collaboration and in lead-lead (Pb–Pb) collisions at $\sqrt{s_{NN}} = 2.76$ and 5.02 TeV from the ALICE Collaboration. In the rest framework of emission source, the probability density function obeyed by meson momenta satisfies the Bose-Einstein distribution, and that obeyed by baryon momenta satisfies the Fermi-Dirac distribution. To simulate the p_T of the charged particles, the kinetic freeze-out temperature T and transverse expansion velocity β_T of emission source are introduced into the relativistic ideal gas model. Our results, based on the Monte Carlo method for numerical calculation, show a good agreement with the experimental data. The excitation functions of T and β_T are then obtained from the analyses, which shows diverse structures from 39 to 62.4 GeV in collisions with different centralities.

Keywords: Multi-source thermal model, Transverse momentum spectra, Bose-Einstein (Fermi-Dirac) distribution, Thermodynamic parameters (characteristics)

PACS: 12.40.Ee, 13.85.Hd, 24.10.Pa

I. INTRODUCTION

The strong interaction, which was used to describe the nuclear force between nucleons (protons or neutrons) at the earliest stage of the universe evolution, is the strongest one [1, 2], being 38 orders of magnitude greater than gravity. As it differs from the atomic and molecular scale interactions, scientists usually use quantum chromodynamics (QCD) to describe the strong interactions between particles below the size of a nucleus [3–5]. In re-

cent years, the research on “new state of matter”, formed in relativistic heavy ion collisions, has attracted many scientists in the field of high energy physics in the world [6].

In extreme conditions, raising the temperature of the system, or increasing its density, the QCD substance will produce two particular phase transitions, one is the deconfinement phase transition and the other is the chiral phase transition [7, 8]. The former corresponds to the disappearance of quark confinement, meaning that quarks are free to move to other regions of the nuclear matter, not just confined to the movement inside the nucleon. The latter corresponds to the restoration of eigensymmetry, that is, the kinetic mass becomes zero and the quarks become as particles, close to zero-mass, while at the same time, the existence of phase transitions indicates the emergence of a new state of matter.

*xhzhang618@163.com; zhang-xuhong@qq.com

†wanghaoning517@139.com

‡Correspondence: fuhuliu@163.com; fuhuliu@sxu.edu.cn

§Correspondence: khkolimov@gmail.com; kh.olimov@uzsci.net

Observation of these two phase transitions in a high-temperature dense region implies the transition of a substance to a state with quark-gluons as the fundamental degree of freedom, and this new state of matter is named quark-gluon plasma (QGP) [9–11]. In QGP expansion, a lot of particles are produced, and finally they are measured in experiments. One may study the formation and change of the new state of matter from the dynamic evolution of the final state particles. Such a matter is usually described by QCD phase diagram [7, 8], and the thermodynamic properties of the system are expressed by the temperature and the chemical potential of the baryons.

When the system undergoes phase transition and reaches the equilibrium state of chemical and kinetic freeze-out stage, the thermodynamic properties of the final state particles can be studied, which is of great significance to obtain the critical point of phase transition and understand the characteristics of QCD. In addition, under low temperature and high density condition, QCD substance will form color superconducting state [12–14] through phase transition. The above two new states of matter do not exist stably, and the heavy ion colliders can be used to control the system state, which provides a powerful tool for researchers to study the QCD phase transition. As an open question, the energy of the critical point is worth studying by various ways [15–19].

Experiments in relativistic heavy ion collisions [20, 21] have provided a new chance for ones to explore new matter and phenomena under extreme conditions. Meanwhile, one may test different theories or models and explain the new effects [22–24]. The whole process of relativistic heavy ion collisions can be divided into three stages: pre-equilibrium dynamics, viscous fluid dynamics, and free flow. In the collisions, a large number of particles are generated and escaped. At the last stage of free flow (i.e. the stage of kinetic freeze-out), as in the relativistic ideal gas model, escaped fermions are subject to Fermi-Dirac statistics and bosons follow the Bose-Einstein statistics. This can be done if one assumes that the generated particles come from the equilibrium stationary source, though the evolution process is represented by a perfect liquid. Due to the extreme squeeze between projectile and target nuclei, a transverse expansion of the interacting system (emission source) or a transverse flow of the final state particles will appear, which affects particle momentum and related quantities in experimental spectra.

In this paper, starting from the probability density function of momenta in the relativistic form, we perform numerical calculations in two steps to analyze the soft

transverse momentum (p_T) spectra of the final state particles generated in high energy gold–gold (Au–Au) and lead–lead (Pb–Pb) collisions measured by the STAR [25–27] and ALICE Collaborations [28, 29], respectively. The thermodynamic parameter T (kinetic freeze-out temperature) and the hydrodynamic parameter β_T (transverse expansion velocity) of the interacting system (emission source) are extracted. In the first step, in the rest frame of emission source, using a parameter T [30–33], the momentum and its each component and energy are sampled according to the assumption of anisotropic emission and a given momentum distribution. In the second step, a new transverse momentum distribution is obtained according to the Lorentz transformation [34] at a given β_T [34–38].

The remainder of this paper is structured as follows. Section 2 introduces the related theoretical distribution and methods of calculations. The comparison and discussion of the results are presented in Section 3. Finally, in Section 4, we summarize and list our main observations and conclusions.

II. FORMALISM AND METHOD

According to the multi-source thermal model [39, 40], many emission sources are assumed to form in high energy collisions. Each stationary emission source emits isotropically particles in various directions. Furthermore, at the kinetic freeze-out, we consider the relativistic ideal gas model [41–43] for the escaped particles in the stationary source. The momentum (p') distribution of the emitted particles obeys the standard distribution [43, 44],

$$f(p') = \frac{1}{N} \frac{dN}{dp'} = Cp'^2 \left[\exp \left(\frac{\sqrt{p'^2 + m_0^2} - \mu}{T} \right) + S \right]^{-1} \quad (1)$$

which is the probability density function. Here, N is the number of particles, $C = (1/m_0^2 kT)[1/K_2(m_0/kT)]$ is the normalization constant, $K_2(m_0/kT)$ is the modified second-order Bessel function correction, $k = 1$ is the Boltzmann constant in the system of natural units, T is the temperature of the emission source, and m_0 and μ are the rest mass and chemical potential of the particle, respectively. When $S = +1, 0$, and -1 , the function corresponds to the Fermi-Dirac distribution, Boltzmann distribution, and Bose-Einstein distribution, respectively [45].

Generally, if $m_0 \gg \mu$, the quantum effect plays a small role, so we can ignore the influence of the chemical potential when studying the momentum distribution in

collisions at higher energy. In case of $m_0 \approx \mu$, the role of the chemical potential increases significantly, and it is necessary for us to distinguish the fermions and bosons. For the case of $m_0 \ll \mu$, the absolute value, $|\sqrt{p'^2 + m_0^2} - \mu|$, should be used to avoid $\sqrt{p'^2 + m_0^2} - \mu < 0$ in low- p' region. In fact, μ is small enough in this work and the case of $\sqrt{p'^2 + m_0^2} - \mu < 0$ does not exist. Although we may regard μ as a free parameter, its value can be obtained in different ways.

Empirically, for baryons, the chemical potential μ_B is given by [46–49],

$$\mu_B = \frac{1.303}{1 + 0.286\sqrt{s_{NN}}}, \quad (2)$$

where $\sqrt{s_{NN}}$ is the collision energy (center-of-mass energy) per nucleon pair, and both μ_B and $\sqrt{s_{NN}}$ are in GeV. Approximately, the chemical potential μ_p of the proton is given by μ_B , and the chemical potential μ_π (μ_K) of the pion (kaon) is taken to be $\mu_\pi = \mu_p m_\pi / m_p$ ($\mu_K = \mu_p m_K / m_p$) by us, where m_π (m_K) is the rest mass of the pion (kaon).

For the convenience of subsequent calculations, we use the Monte Carlo method [5, 50, 51] to obtain the momentum distribution and discrete values of each component and energy. Let $R_{1,2,3}$ be random numbers that follow a uniform distribution in the range of $[0, 1]$. For a discrete p' , it satisfies the momentum sampling:

$$\int_0^{p'} f(p'') dp'' < R_1 < \int_0^{p' + \delta p'} f(p'') dp'', \quad (3)$$

where $\delta p'$ is a small shift from p' and $f(p'')$ is just Eq. (1). The azimuthal angle of the isotropic emission is obtained by

$$\varphi' = 2\pi R_2, \quad (4)$$

and the emission angle is

$$\vartheta' = 2 \arcsin \sqrt{R_3}. \quad (5)$$

Thus, in the rectangular coordinate system $O-xyz$, where Oz axis is the beam direction and xOz plane is the reaction plane, one obtains the x -component of the momentum,

$$p'_x = p' \sin \vartheta' \cos \varphi', \quad (6)$$

and the y -component of the momentum,

$$p'_y = p' \sin \vartheta' \sin \varphi', \quad (7)$$

the transverse momentum,

$$p'_T = p' \sin \theta', \quad (8)$$

the z -component of the momentum,

$$p'_z = p' \cos \theta', \quad (9)$$

and the energy,

$$E' = \sqrt{p'^2 + m_0^2}. \quad (10)$$

Now we consider the Lorentz transformation from the stationary source to the expanding one, which is caused by the interactions among multiple sources. Let $\beta_{x,y,z}$ denote the components of the expansion velocity. We have

$$p_x = \frac{1}{\sqrt{1 - \beta_x^2}} (p'_x + \beta_x E'), \quad (11)$$

$$p_y = \frac{1}{\sqrt{1 - \beta_y^2}} (p'_y + \beta_y E'), \quad (12)$$

and

$$p_z = \frac{1}{\sqrt{1 - \beta_z^2}} (p'_z + \beta_z E'). \quad (13)$$

The transverse momentum is given by

$$p_T = \sqrt{p_x^2 + p_y^2} = \frac{1}{\sqrt{(1 - \beta_x^2)(1 - \beta_y^2)}} \times \sqrt{(1 - \beta_y^2)(p'_x + \beta_x E')^2 + (1 - \beta_x^2)(p'_y + \beta_y E')^2}. \quad (14)$$

Here, $\sqrt{\beta_x^2 + \beta_y^2} = \beta_T$. Due to the small difference between β_x and β_y , we ignore this difference and take $\beta_x = \beta_y$ for simplicity when describing the transverse momentum spectrum. It should be noted that the difference cannot be ignored in analyzing anisotropic flow.

It should be noted that Eq. (13) contains only the proper expansion, but not the longitudinal expansion or motion of the emission source. If the longitudinal effect is considered, we may use a larger β_z in Eq. (13). In this case, the “expansion” of emission source is anisotropic in the three dimensional momentum space, though the expansion can be taken to be isotropic in the transverse plane when the transverse anisotropic flow is not the topic of the present work.

III. RESULTS AND DISCUSSION

A. Comparison with data

We collected a large number of transverse momentum spectra of the final state particles generated in Au–Au and Pb–Pb collisions over an energy range from 7.7

GeV to 5.02 TeV, measured by the STAR [25–27] and ALICE [28, 29] Collaborations, and then performed a fitting analysis on them in Figures 1–3. In order to compare the properties of the p_T spectra at all energies more comprehensively, we limit the range of p_T to be equal to or less than 3 GeV/ c , which falls into the soft p_T region. Different symbols represent the experimental data in different centrality classes, and the curves are our results calculated by the Monte Carlo method. In addition, for showing p_T spectra more clearly in different centrality classes, we indented the data to the power of 10 (such as the numbers in parentheses in the legend). The length of the gray rectangle in the figure represents the error of p_T , and the width represents the error of p_T spectrum $[(1/2\pi p_T)d^2N/dydp_T]$, which is the quadratic sum of the statistical and systematic uncertainties.

Figure 1 shows the result of fitting analysis of p_T spectra of negatively and positively charged pions (π^- and π^+) from central (0–5%) to peripheral (70–80%) collisions using the Bose-Einstein distribution embedded an expansion velocity. Panels (a)–(j) represent the p_T spectra at different collision energies shown in the figure. The closed (open) symbols and solid (dashed) curves correspond to π^- (π^+), and there is no distinction between π^- and π^+ in panel (j). The experimental data presented in panels (a)–(h) are quoted from the STAR Collaboration for Au–Au collisions, which shows the mid-rapidity range of $|y| < 0.1$ [25–27]; and the experimental data presented in panels (i) and (j) are collected from ALICE Collaboration for Pb–Pb collisions, whose mid-(pseudo)rapidity range is $|y| < 0.5$ [28] and $|\eta| < 0.8$ [29]. The values of the free parameters T and β_T extracted from the fits will be analyzed in next subsection. Following each panel, the ratios of Data/Fit are given to show the quality of the fit.

Similar to Figure 1, Figures 2 and 3 show the p_T spectra of negative and positive kaons (K^- , K^+ , or $K^- + K^+$) and anti-protons and protons (\bar{p} , p , or $\bar{p} + p$) respectively [25–29], where the spectra in Figure 2 are fitted with the Bose-Einstein distribution with embedded transverse expansion velocity and the spectra in Figure 3 are fitted with the Fermi-Dirac distribution with embedded transverse expansion velocity. The related parameters will be analyzed in next subsection.

From Figures 1–3 one can see that the Bose-Einstein/Fermi-Dirac distribution with embedded transverse expansion velocity can describe the soft p_T spectra of light charged particles produced in high-energy Au–Au and Pb–Pb collisions at the Relativistic Heavy Ion Collider and the Large Hadron Collider. In the description,

there are only two free parameters: the kinetic freeze-out temperature T and the transverse expansion velocity β_T . Compared with the general treatments in the community, the present work has used a more clear picture and a simpler distribution. In fact, the Bose-Einstein/Fermi-Dirac distribution is the most basic one in the ideal gas model.

From the ratios of Data/Fit, one can see that in very low p_T region and around $p_T \approx 3$ GeV/ c , the fitting results underestimate the data in some cases. This means that we need a very soft component for the contribution of resonance decay. Meanwhile, we need a hard component for the contribution of hard scattering process. Naturally, a multi-component distribution can be applied for the whole p_T region. Although other methods can describe the p_T spectra, the present work provides an alternative method in the description. It does have clear picture and methodological significance.

B. Tendencies of parameters

Figure 4 shows the dependence of T on the collision energy $\sqrt{s_{NN}}$, centrality class (percentage), and particle mass. From panels (a) to (i), the centrality classes are 0–5%, 5–10%, ..., 70–80%, respectively. The closed (open) squares, circles, and triangles represent the results for π^- (π^+), K^- (K^+), and \bar{p} (p), respectively. The weighted averages over the yields of different particles are shown by the crosses. One can see that T increases generally with the increase of collision energy. There is a large variation of T from 39 to 62.4 GeV in central collisions. The variation becomes small in semi-central collisions and disappears in peripheral collisions. From central to peripheral collisions, T has a slight decrease. In central collisions, T increases with the increase of particle mass, and in peripheral collisions the situation seems to be different or ambiguous. The dependence of T on isospin is not significant.

Figure 5 is similar to Figure 4, but it shows the dependence of β_T on the collision energy, centrality class, and particle mass. One can see that β_T increases generally with the increase of collision energy. There is a large change in the slope from 39 to 62.4 GeV and from 200 to 2760 GeV in collisions with different centralities. From central to peripheral collisions, β_T has a slight decrease. In central collisions, β_T does not change significantly with the increase of particle mass, and in peripheral collisions, β_T decreases with the increase of particle mass. The difference between β_T from the spectra of negative and

positive particles decreases with the particle mass. Compared with T , β_T shows larger fluctuations in the spectra, which is reflected by its errors.

It should be noted that the dependence of T on centrality is an open question at present, though β_T increases with the increase of centrality. Based on the blast-wave model [35], the ALICE Collaboration [28] shows that T decreases slightly with the increase of centrality. However, our results show that T increases slightly with the increase of centrality. The difference is caused by different methods which also lead to different values in parameters. In the blast-wave model [35], a self-similar and variant flow profile function is used. In the present work, we have used an invariant flow velocity. In central collisions, although a lower temperature can be explained by a longer lifetime of the system, a higher temperature can be explained by a higher excitation degree.

C. Further discussions

Generally, the interacting system of relativistic heavy ion collisions [20, 21] will experience two stages of freeze-out, one is chemical freeze-out and the other is kinetic freeze-out. The two kinds of freeze-outs possibly occur simultaneously or non-simultaneously. It depends on the sizes of chemical and kinetic freeze-out temperatures. In fact, the system is suddenly frozen [52, 53] and the short-lived resonances decay [54], changing the kinetic spectra of stable particles. The resonances of the system, generated during chemical freeze-out, decay rapidly, but the system continues to evolve with elastic collisions between hadrons, and the system will stay in the local thermal equilibrium before kinetic freeze-out [55]. The particles' transverse momentum spectra carry information about it.

If the chemical and kinetic freeze-out temperatures are nearly the same, one may consider that the two freeze-outs occur almost simultaneously. If the two freeze-outs occur at different time moments, the chemical freeze-out happens generally earlier than the kinetic freeze-out, and the chemical freeze-out temperature is larger than the kinetic one. The temperature T extracted from the present work is only the kinetic freeze-out temperature. The chemical freeze-out temperature is not available here, and we cannot give a comparison for the two temperatures corresponding to the two freeze-outs.

Studying the transverse momentum (mass) spectra of the final state particles, produced in relativistic heavy

ion collisions, is an effective and fast means to obtain thermodynamic parameters of the system. The emission source determines the transverse momentum spectra of different kinds of particles. When the interacting system is in the stage of kinetic freeze-out, the emitted particles not only contain thermal motion, but also are affected by the expansion of the system or the flow velocity of the particles. Thermal motion reflects the transverse excitation degree of the system, which can be reflected by the kinetic freeze-out temperature T . The expansion or flow effect embodies the hydrodynamic feature of the system, which can be represented by the transverse expansion or flow velocity β_T .

In the community, the transverse momentum spectra have been studied extensively for different final state particles. The functions usually used in fitting the transverse momentum spectra include the Tsallis distribution [56–58], the Erlang distribution [59–61], the Hagedorn function [62, 63], etc. In the present work, we have adopted the most basic function, the Bose-Einstein/Fermi-Dirac distribution, in the relativistic ideal gas model and introduced the transverse expansion velocity of the system to analyze and fit the transverse momentum spectra of the charged particles, π^- , π^+ , K^- , K^+ , \bar{p} , and p produced in Au–Au and Pb–Pb collisions at high energies, and obtain the thermodynamic parameter T and the hydrodynamic parameter β_T .

Our work shows that the excitation functions of T and β_T display some particular changes from 39 to 62.4 GeV. This possibly means that the interacting system undergoes a change of reaction mechanism or generated matter. This change could be a signature of the deconfinement phase transition from hadronic matter to QGP. Because the most basic function, the Bose-Einstein/Fermi-Dirac distribution, in the relativistic ideal gas model is used, and the transverse expansion velocity of the system is introduced, we consider that the present work has a more solid foundation than the other distributions or functions used in the community. Moreover, there are only two free parameters in the description of transverse momentum spectra, which is also an advantage of the present work.

IV. SUMMARY AND CONCLUSIONS

Based on the framework of a multi-source thermal model, we have analyzed the soft transverse momentum spectra of π^- , π^+ , K^- , K^+ , \bar{p} , and p produced in Au–Au collisions at $\sqrt{s_{NN}} = 7.7, 11.5, 14.5, 19.6, 27, 39, 62.4$, and 200 GeV, measured by the STAR Collaboration, and

in Pb–Pb collisions at $\sqrt{s_{NN}} = 2.76$ and 5.02 TeV, measured by the ALICE Collaboration. In the rest frame-work of emission source, the probability density function of meson momenta satisfies the Bose-Einstein distribution, and that of baryon momenta satisfies the Fermi-Dirac distribution.

Considering the interactions among multiple sources, the emission source has an expansion velocity or the particles have a flow velocity. To simulate the transverse momentum spectra, the kinetic freeze-out temperature and transverse expansion velocity of emission source are introduced. The numerical results, calculated by the Monte Carlo method, are in good agreement with the experimental data of the STAR and ALICE Collaborations. The excitation function, and the centrality and particle mass dependences of kinetic freeze-out temperature and transverse expansion velocity are obtained from the analyses.

With the increase of collision energy, the kinetic freeze-out temperature increases generally. There is a large variation of the temperature from 39 to 62.4 GeV in central collisions. The variation becomes small in semi-central collisions and disappears in peripheral collisions. From central to peripheral collisions, the kinetic freeze-out temperature has a slight decrease. In central collisions, the kinetic freeze-out temperature increases with the increase of particle mass, and in peripheral collisions the situation seems to be different or ambiguous.

The transverse expansion velocity increases generally with the increase of collision energy. There is a large change in the slope from 39 to 62.4 GeV in collisions with different centralities. From central to peripheral collisions, the transverse expansion velocity has a slight decrease. In central collisions, the transverse expansion velocity does not change significantly with the increase of particle mass, and in peripheral collisions the transverse expansion velocity decreases with the increase of particle mass.

Compared with the kinetic freeze-out temperature, the transverse expansion velocity shows larger fluctuations in the spectra, which implies that the introduction of transverse expansion velocity is indeed necessary. The fact that the excitation functions of the free parameters display some particular changes from 39 to 62.4 GeV

possibly implies that the interacting system undergoes the process of transition of the hadronic matter into QGP. Being the most basic function, the Bose-Einstein/Fermi-Dirac distribution with the introduced transverse expansion velocity implies that the present work has a solid foundation.

Data Availability

The data used to support the findings of this study are included within the article and are cited at relevant places within the text as references.

Ethical Approval

The authors declare that they are in compliance with ethical standards regarding the content of this paper.

Disclosure

The funding agencies have no role in the design of the study; in the collection, analysis, or interpretation of the data; in the writing of the manuscript; or in the decision to publish the results.

Conflicts of Interest

The authors declare that there are no conflicts of interest regarding the publication of this paper.

Acknowledgments

The work of X.-H.Z. was supported by the Innovative Foundation for Graduate Education in Shanxi University. The work of Shanxi Group was supported by the National Natural Science Foundation of China under Grant Nos. 12147215, 12047571, and 11575103, the Shanxi Provincial Natural Science Foundation under Grant Nos. 202103021224036 and 201901D111043, the Scientific and Technological Innovation Programs of Higher Education Institutions in Shanxi (STIP) under Grant No. 201802017, and the Fund for Shanxi “1331 Project” Key Subjects Construction. The work of Kh.K.O. was supported by the Ministry of Innovative Development of the Republic of Uzbekistan within the fundamental project No. F3-20200929146 on analysis of open data on heavy-ion collisions at RHIC and LHC.

[1] Z. W. Lin and M. Gyulassy, “Open charm as a probe of preequilibrium dynamics in nuclear collisions?,” *Physical Review C*, vol. 51, pp. 2177–2187, 1995.

[2] M. Cacciari, P. Nason, and R. Vogt, “QCD predictions for charm and bottom quark production at RHIC,” *Physical Review Letters*, vol. 95, article 122001, 2005.

- [3] D. Kharzeev and K. Tuchin, “Bulk viscosity of QCD matter near the critical temperature,” *Journal of High Energy Physics*, vol. 2008, no. 9, article 093, 2008.
- [4] F. Karsch, D. Kharzeev, and K. Tuchin, “Universal properties of bulk viscosity near the QCD phase transition,” *Physics Letters B*, vol. 663, pp. 217–221, 2008.
- [5] C. P. Robert and G. Casella, *Monte Carlo Statistical Methods*, Springer Press, New York, 2nd edition, 2004.
- [6] C. Shen, Z. Qiu, H.-C. Song, J. Bernhard, and S. Bass “The iEBE-VISHNU code package for relativistic heavy-ion collisions,” *Computer Physics Communications*, vol. 199, pp. 61–85, 2016.
- [7] B. Mohanty, “Exploring the quantum chromodynamics landscape with high-energy nuclear collisions,” *New Journal of Physics*, vol. 13, article 065031, 2011.
- [8] P. Braun-Munzinger and J. Wambach, “Colloquium: Phase diagram of strongly interacting matter,” *Review of Modern Physics*, vol. 2009, pp. 1031–1050, 2009.
- [9] H. Satz and R. Stock, “Quark matter: The beginning,” *Nuclear Physics A*, vol. 956, pp. 898–901, 2016.
- [10] B. Liu, M. Di Toro, G. Y. Shao, V. Greco, C. W. Shen, and Z. H. Li, “Hadron-quark phase coexistence in a hybrid MIT-bag model,” *The European Physical Journal A*, vol. 47, article 104, 2011.
- [11] H. Bohr, and H.B. Nielsen, “Hadron production from a boiling quark soup: A thermodynamical quark model predicting particle ratios in hadronic collisions,” *Nuclear Physics B*, vol. 128, pp. 275–293, 1977.
- [12] M. Alford, J. A. Bowers, and K. Rajagopal, “Crystalline color superconductivity,” *Physical Review D*, vol. 63, article 074016, 2001.
- [13] M. Huang and I. A. Shovkovy, “Screening masses in a neutral two-flavor color superconductor,” *Physical Review D*, vol. 70, article 094030, 2004.
- [14] P. F. Bedaque, H. Caldas, and G. Rupak, “Phase separation in Asymmetrical fermion superfluids,” *Physical Review Letters*, vol. 91, article 247002, 2003.
- [15] X. F. Luo for the STAR Collaboration, “Search for the QCD critical point by higher moments of net-proton multiplicity distributions at STAR,” *Nuclear Physics A*, vol. 904–905, pp. 911c–914c, 2013.
- [16] P. Tribedy for the STAR Collaboration, “Search for QCD phase transitions and the critical point utilizing particle ratio fluctuations and transverse momentum correlations from the STAR experiment,” *Nuclear Physics A*, vol. 904–905, pp. 463c–466c, 2013.
- [17] N. R. Sahoo for the STAR Collaboration, “Recent results on event-by-event fluctuations from the RHIC Beam Energy Scan program in the STAR experiment,” *Journal of Physics: Conference Series*, vol. 535, article 012007, 2014.
- [18] M. S. Abdallah, B. E. Aboona, J. Adam et al. (STAR Collaboration), “Measurements of proton high-order cumulants in $\sqrt{s_{NN}} = 3$ GeV Au+Au collisions and implications for the QCD critical point,” *Physical Review Letters*, vol. 128, article 202303, 2022.
- [19] Z. B. Tang, Y. C. Xu, L. J. Ruan, G. V. Buren, F. Q. Wang, Z. B. Xu, “Spectra and radial flow in relativistic heavy ion collisions with Tsallis statistics in a blast-wave description,” *Physical Review C*, vol. 79, article 051901(R), 2009.
- [20] K. Adcox, S. S. Adler, S. Afanasiev et al. (PHENIX Collaboration), “Formation of dense partonic matter in relativistic nucleus-nucleus collisions at RHIC: Experimental evaluation by the PHENIX Collaboration,” *Nuclear Physics A*, vol. 757, pp. 184–283, 2005.
- [21] J. Adams, M. M. Aggarwal, Z. Ahammed et al. (STAR Collaboration), “Experimental and theoretical challenges in the search for the quark-gluon plasma: The STAR Collaboration’s critical assessment of the evidence from RHIC collisions,” *Nuclear Physics A*, vol. 757, pp. 102–183, 2005.
- [22] N. Xu (for the STAR Collaboration) “An overview of STAR experimental results,” *Nuclear Physics A*, vol. 931, pp. 1–12, 2014.
- [23] A. Andronic, P. Braun-Munzinger, K. Redlich, and J. Stachel “Decoding the phase structure of QCD via particle production at high energy,” *Nature*, vol. 561, pp. 321–330, 2018.
- [24] S. Gupta, X.-F. Luo, B. Mohanty, H. G. Ritter, and N. Xu “Scale for the phase diagram of quantum chromodynamics,” *Science*, vol. 332, pp. 1525–1528, 2011.
- [25] L. Adamczyk, J. K. Adkins, G. Agakishiev et al. (STAR Collaboration), “Bulk properties of the medium produced in relativistic heavy-ion collisions from the beam energy scan program,” *Physical Review C*, vol. 96, article 044904, 2017.
- [26] J. Adam, L. Adamczyk, J. R. Adams et al. (STAR Collaboration), “Bulk properties of the system formed in Au+Au collisions at $\sqrt{s_{NN}} = 14.5$ GeV at the BNL STAR detector,” *Physical Review C*, vol. 101, article 024905, 2020.
- [27] B. I. Abelev, M. M. Aggarwal, Z. Ahammed et al. (STAR Collaboration), “Systematic measurements of identified particle spectra in pp , $d+Au$, and $Au+Au$ collisions at the STAR detector,” *Physical Review C*, vol. 79, article 034909, 2009.
- [28] B. Abelev, J. Adam, D. Adamová et al. (ALICE Collaboration), “Centrality dependence of π , K , and p production in Pb-Pb collisions at $\sqrt{s_{NN}} = 2.76$ TeV,” *Physical Review C*, vol. 88, article 044910, 2013.
- [29] S. Acharya, D. Adamová, S. P. Adhya et al. (ALICE Collaboration), “Production of charged pions, kaons and (anti-)protons in Pb-Pb and inelastic pp collisions at $\sqrt{s_{NN}} = 5.02$ TeV,” *Physical Review C*, vol. 101, arti-

- cle 044907, 2020.
- [30] G. Wilk and Z. Włodarczyk, “Consequences of temperature fluctuations in observables measured in high-energy collisions,” *The European Physical Journal A*, vol. 48, article 161, 2012.
 - [31] T. S. Biró, G. G. Barnaföldi, G. Biró, and K. M. Shen, “Near and far from equilibrium power-law statistics,” *Journal of Physics: Conference Series*, vol. 779, article 012081, 2017.
 - [32] G. Wilk and Z. Włodarczyk, “Interpretation of nonextensivity parameter q in some applications of Tsallis statistics and Lévy distributions,” *Physical Review Letters*, vol. 84, article 2770, 2000.
 - [33] T. S. Biró, P. Ván, G. G. Barnaföldi, and K. Ürmösy, “Statistical power law due to reservoir fluctuations and the universal thermostat independence principle,” *Entropy*, vol. 16, pp. 6497–6514, 2014.
 - [34] H. Niemi, K. J. Eskola, and R. Paatelainen “Event-by-event fluctuations in a perturbative QCD + saturation + hydrodynamics model: Determining QCD matter shear viscosity in ultrarelativistic heavy-ion collisions,” *Physical Review C*, vol. 93, article 024907, 2016.
 - [35] E. Schnedermann, J. Sollfrank, and U. Heinz, “Thermal phenomenology of hadrons from 200A GeV S+S collisions,” *Physical Review C*, vol. 48, pp. 2462–2475, 1993.
 - [36] M. Waqas and B.-C. Li, “Kinetic freeze-out temperature and transverse flow velocity in Au-Au collisions at RHIC-BES energies,” *Advances in High Energy Physics*, vol. 2020, article 1787183, 2020.
 - [37] K. J. Eskola, H. Niemi and R. Paatelainen, “Pinning down QCD-matter shear viscosity in ultrarelativistic heavy-ion collisions via EbyE fluctuations using pQCD + saturation + hydrodynamics,” *Nuclear and Particle Physics Proceedings*, vol. 276–278, pp. 161–164, 2016.
 - [38] F.-H. Liu and H.-L. Lao, “Blast-wave revision of the multisource thermal model in nucleus-nucleus collisions,” *Indian Journal of Physics*, vol. 90, pp. 1077–1085, 2016.
 - [39] F.-H. Liu, N. N. Abd Allah, and B. K. Singh “Dependence of black fragment azimuthal and projected angular distributions on polar angle in silicon-emulsion collisions at 4.5A GeV/c,” *Physical Review C*, vol. 69, article 057601, 2004.
 - [40] F.-H. Liu, C.-X. Tian, M. -Y. Duan, and B.-C. Li “Relativistic and quantum revisions of the multisource thermal model in high-energy collisions,” *Advances in High Energy Physics*, vol. 2012, article 287521, 2012.
 - [41] J. Cleymans and D. Worku, “Relativistic thermodynamics: Transverse momentum distributions in high-energy physics,” *The European Physical Journal A*, vol. 48, article 160, 2012.
 - [42] P. N. Pandita, “Critical behavior of a relativistic bose gas,” *Physical Review E*, vol. 89, article 032110, 2014.
 - [43] C. D. Dermer “The production spectrum of a relativistic Maxwell-Boltzmann gas,” *The Astrophysical Journal*, vol. 280, pp. 328–333, 1984.
 - [44] C. R. Meng, “Transverse momentum and rapidity distributions of ϕ mesons produced in Pb-Pb collisions at SPS energies,” *Chinese Physics Letters*, vol. 26, article 102501, 2009.
 - [45] P. Z. Ning, L. Li, and D. F. Min, Foundation of Nuclear Physics: Nucleons and Nuclei, Higher Education Press, Beijing, China, 2003.
 - [46] A. Andronic, P. Braum-Munzinger, and J. Stachel, “The horn, the hadron mass spectrum and the QCD phase diagram - the statistical model of hadron production in central nucleus-nucleus collisions,” *Nuclear Physics A*, vol. 834, pp. 237c–240c, 2010.
 - [47] A. Andronic, P. Braum-Munzinger, and J. Stachel, “Hadron production in central nucleus-nucleus collisions at chemical freeze-out,” *Nuclear Physics A*, vol. 772, pp. 167–199, 2006.
 - [48] A. Andronic, P. Braum-Munzinger, and J. Stachel, “Thermal hadron production in relativistic nuclear collisions,” *Acta Physica Polonica B*, vol. 40, pp. 1005–1012, 2009.
 - [49] J. Cleymans, H. Oeschler, K. Redlich, and S. Wheaton, “Comparison of chemical freeze-out criteria in heavy-ion collisions,” *Physical Review C*, vol. 73, article 034905, 2006.
 - [50] N. Metropolis and S. Ulam, “The Monte Carlo method,” *Journal of the American Statistical Association*, vol. 44, pp. 335–341, 1949.
 - [51] D. E. Raeside, “Monte Carlo principles and applications,” *Physics in Medicine & Biology*, vol. 21, pp. 181–197, 1976.
 - [52] W. Broniowski and W. Florkowski, “Description of the RHIC p_{\perp} spectra in a thermal model with expansion,” *Physical Review Letters*, vol. 87, article 272302, 2001.
 - [53] A. Motornenko, V. Vovchenko, C. Greiner, and H. Stoecker, “Kinetic freeze-out temperature from yields of short-lived resonances,” *Physical Review C*, vol. 102, article 024909, 2020.
 - [54] A. Mazeliauskas and V. Viskavicius, “Temperature and fluid velocity on the freeze-out surface from π , K , and p spectra in pp , p -Pb, and Pb-Pb collisions,” *Physical Review C*, vol. 101, article 014910, 2020.
 - [55] J. Chen, J. Deng, Z. B. Tang, Z. B. Xu, and L. Yi, “Nonequilibrium kinetic freeze-out properties in relativistic heavy ion collisions from energies employed at the RHIC beam energy scan to those available at the LHC,” *Physical Review C*, vol. 104, article 034901, 2021.
 - [56] H. Zheng and L. L. Zhu, “Can Tsallis distribution fit all the particle spectra produced at RHIC and LHC?,” *Advances in High Energy Physics*, vol. 2015, article 180491, 2015.

- 2020.
- [57] H. Zheng, L. L. Zhu, and A. Bonasera, “Systematic analysis of hadron spectra in $p+p$ collisions using Tsallis distributions,” *Physical Review D*, vol. 92, article 074009, 2015.
 - [58] S. Charchyan, V. Khachatryan, A. M. Sirunyan et al. (CMS Collaboration), “Study of the inclusive production of charged pions, kaons, and protons in pp collisions at $\sqrt{s} = 0.9, 2.76$, and 7 TeV,” *The European Physical Journal C*, vol. 72, article 2164, 2012.
 - [59] F.-H. Liu and J.-S. Li, “Isotopic production cross section of fragments in $^{56}\text{Fe}+p$ and $^{136}\text{Xe}(^{124}\text{Xe})+\text{Pb}$ reactions over an energy range from 300A to 1500A MeV,” *Physical Review C*, vol 78, article 044602, 2008.
 - [60] F.-H. Liu, “Unified description of multiplicity distributions of final-state particles produced in collisions at high energies,” *Nuclear Physics A*, vol. 810, pp. 159–172, 2008.
 - [61] F.-H. Liu, Y.-Q. Gao, T. Tian, and B.-C. Li, “Unified description of transverse momentum spectrums contributed by soft and hard processes in high energy nuclear collisions,” *The European Physical Journal A*, vol. 50, article 94, 2014.
 - [62] B. Abelev, J. Adam, D. Adamová et al. (ALICE Collaboration), “Production of $\Sigma(1385)^\pm$ and $\Xi(1530)^0$ in proton-proton collisions at $\sqrt{s}=7$ TeV,” *The European Physical Journal C*, vol. 75, article 1, 2015.
 - [63] H. Hagedorn, “Multiplicities, p_T distributions and the expected hadron \rightarrow quark-gluon phase transition,” *La Rivista del Nuovo Cimento*, vol. 6, no. 10, pp. 1–50, 1983.

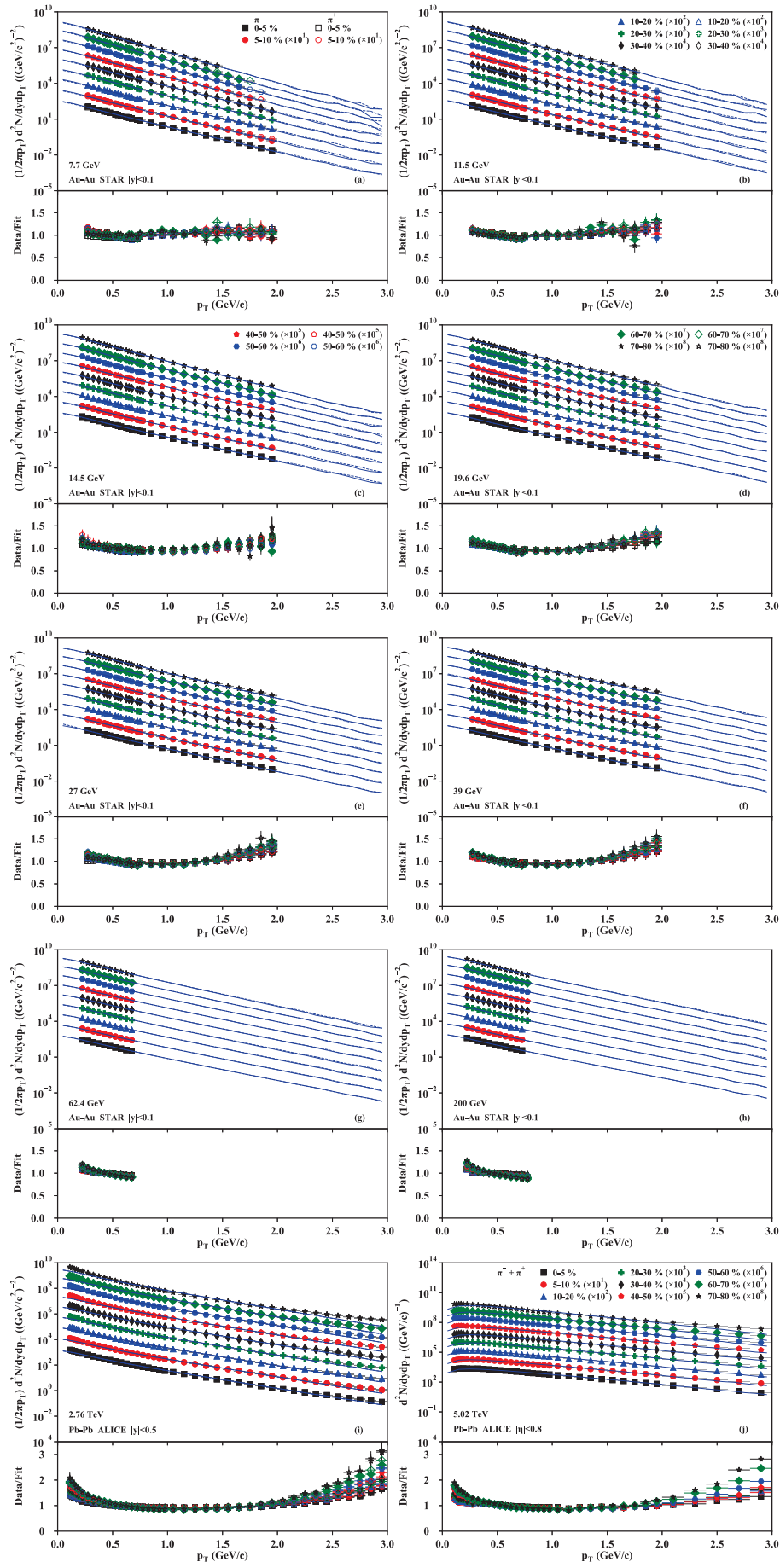


Figure 1. Transverse momentum spectra of π^- and π^+ produced in Au–Au collisions at $\sqrt{s_{NN}} = 7.7$ GeV (a), 11.5 GeV (b), 14.5 GeV (c), 19.6 GeV (d), 27 GeV (e), 39 GeV (f), 62.4 GeV (g), and 200 GeV (h), as well as in Pb–Pb collisions at 2.76 TeV (i) and 5.02 TeV (j) with various centrality classes and given mid-rapidity. The symbols represent the experimental data measured by the STAR [25–27] and ALICE [28, 29] Collaborations and re-scaled by different amounts marked in the panels. The curves are our results fitted by the Bose-Einstein distribution with embedded transverse expansion velocity.

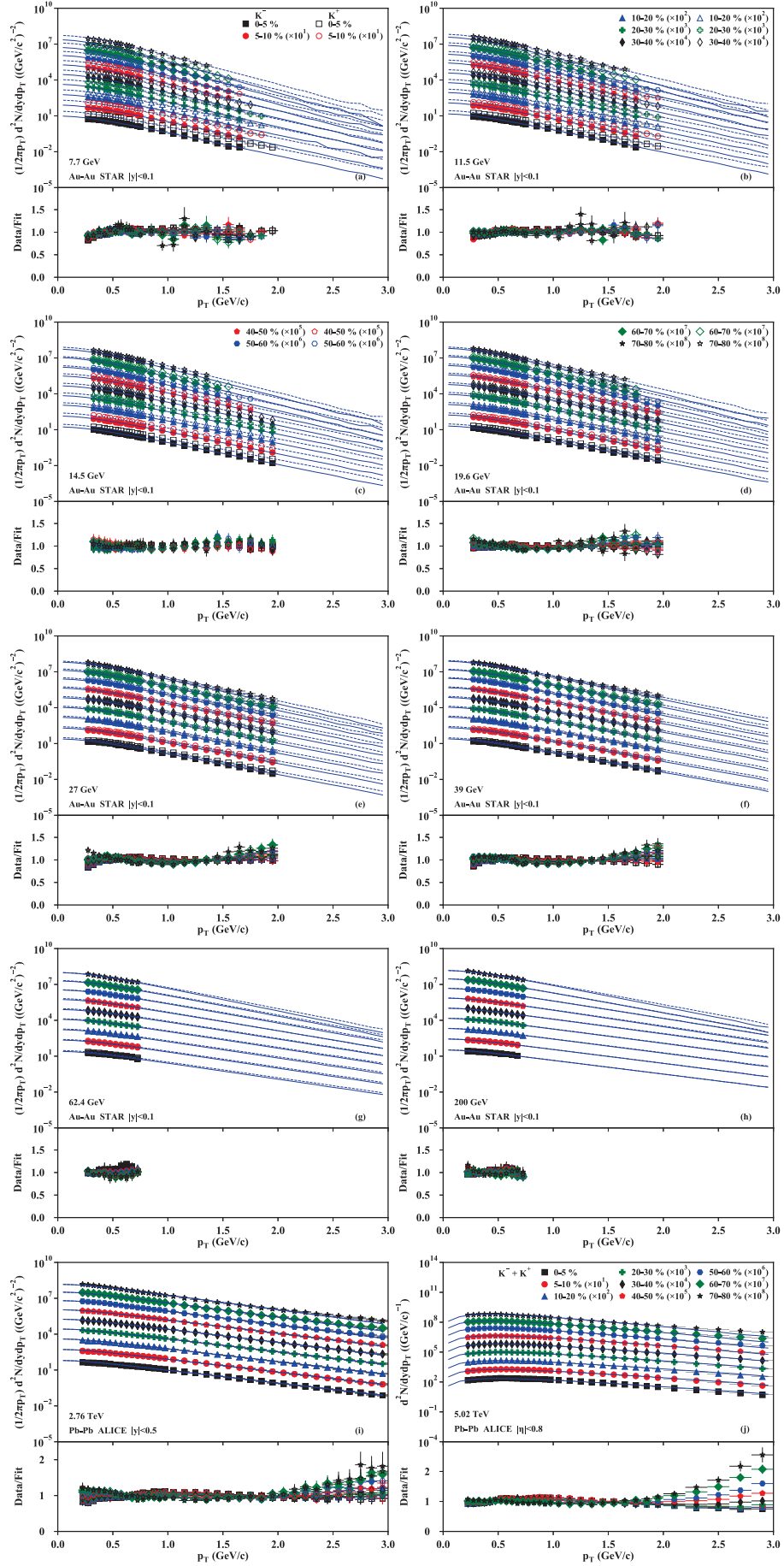


Figure 2. Same as Figure 1, but showing the transverse momentum spectra of K^- and K^+ . The curves are our results fitted by the Bose-Einstein distribution with embedded transverse expansion velocity.

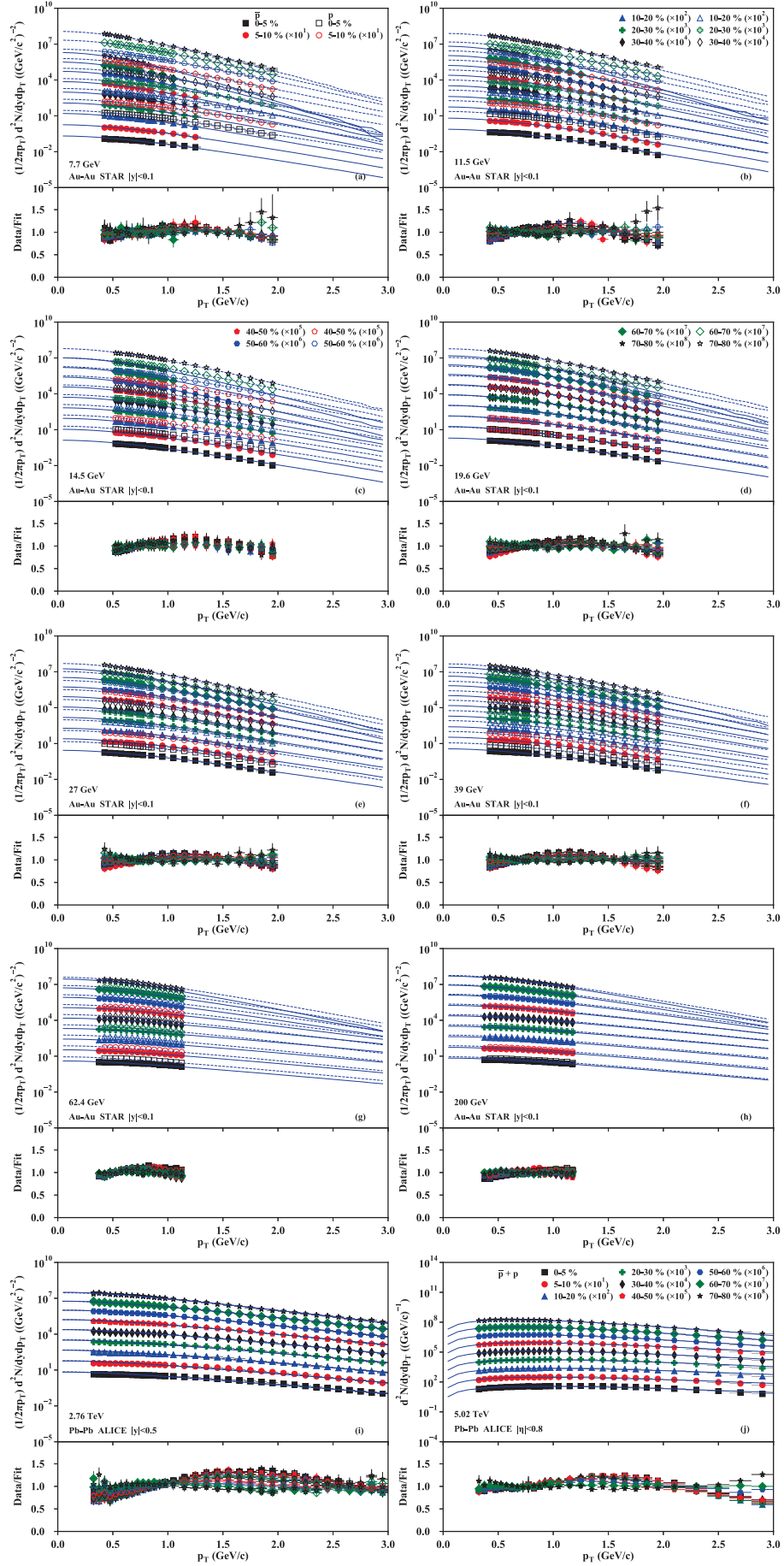


Figure 3. Same as Figure 1, but showing the transverse momentum spectra of \bar{p} and p . The curves are our results fitted by the Fermi-Dirac distribution with embedded transverse expansion velocity.

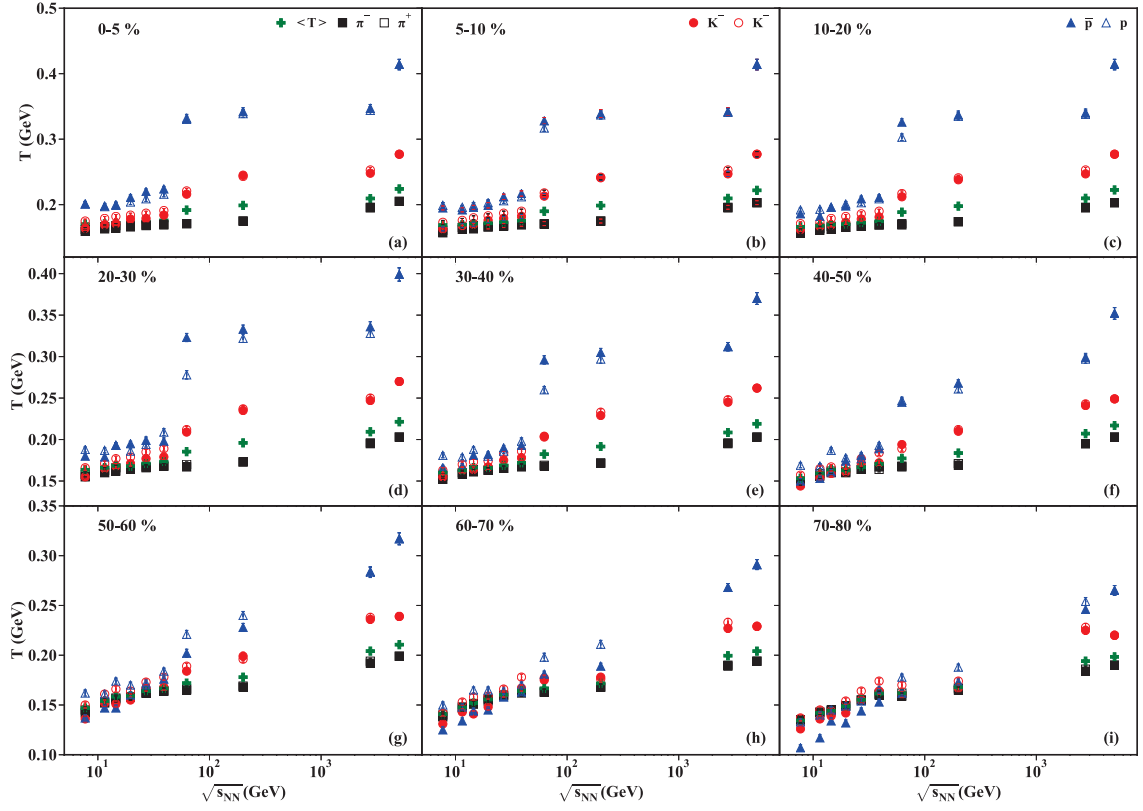


Figure 4. Dependence of the kinetic freeze-out temperature T on the collision energy $\sqrt{s_{NN}}$, centrality, and particle mass or type. From panels (a) to (i), the centrality classes are 0–5%, 5–10%, ..., and 70–80%, respectively. The closed (open) squares, circles, and triangles represent the results for π^- (π^+), K^- (K^+), and \bar{p} (p), respectively, where the closed symbols at 5.02 TeV are not undistinguished the charges. The crosses represent the average T ($\langle T \rangle$) weighted over the yields of different particles. All symbols represent the results fitted from Figures 1–3.

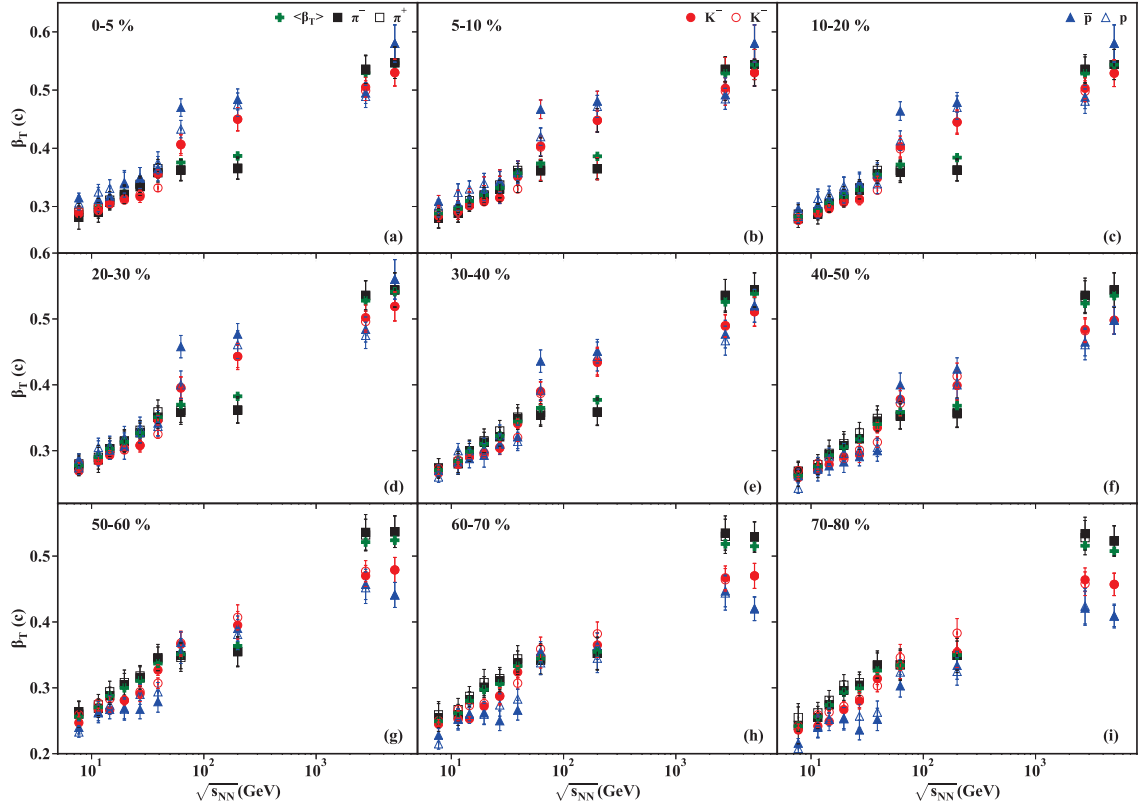


Figure 5. Same as Figure 4, but showing the dependence of the transverse expansion velocity β_T on the collision energy $\sqrt{s_{NN}}$, centrality, and particle mass. The average β_T ($\langle \beta_T \rangle$) is the weighted average over the yields of different particles.